



Combined visual and biochemical analyses confirm depositor and diet for Neolithic coprolites from Skara Brae

Andrzej A. Romaniuk^{1,2} · Elsa Panciroli^{2,3,4} · Michael Buckley⁵ · Manasij Pal Chowdhury⁵ · Carla Willars⁶ · Jeremy S. Herman² · Lore G. Troalen⁷ · Alexandra N. Shepherd⁸ · David V. Clarke⁹ · Alison Sheridan⁹ · Bart E. van Dongen⁵ · Ian B. Butler³ · Robin Bendrey¹

Received: 7 May 2020 / Accepted: 11 October 2020 / Published online: 10 November 2020

© The Author(s) 2020

Abstract

Coprolites (fossilized faeces) can provide valuable insights into species' diet and related habits. In archaeozoological contexts, they are a potential source of information on human-animal interactions as well as human and animal subsistence. However, despite a broad discussion on coprolites in archaeology, such finds are rarely subject to detailed examination by researchers, perhaps due to the destructive nature of traditional analytical methods. Here, we have examined coprolitic remains from the Neolithic (third millennium BCE) settlement at Skara Brae, Orkney, using a range of modern methods: X-ray computed tomography, scanning electron microscopy, lipid and protein analysis (shotgun proteomics of the coprolite matrix as well as collagen peptide mass fingerprinting of isolated bone fragments). This combined approach minimised destructiveness of sampling, leaving sufficient material for subsequent study, while providing more information than traditional morphological examination alone. Based on gross visual examination, coprolites were predominantly attributed to domestic dogs (*Canis familiaris*), with morphologically identified bone inclusions derived from domestic sheep (*Ovis aries*) and common voles (*Microtus arvalis*). Partial dissection of a coprolite provided bone samples containing protein markers akin to those of domestic sheep. Considering the predominance of vertebral and distal limb bone fragments, Skara Brae dogs were probably consuming human butchery or meal refuse, either routinely fed to them or scavenged. The presumably opportunistic consumption of rodents may also have played a role in pest control.

Keywords Neolithic · Coprolite · Diet · X-ray computed tomography · Mass spectrometry · Scanning electron microscopy

Supplementary Information The online version of this article (<https://doi.org/10.1007/s12520-020-01225-9>) contains supplementary material, which is available to authorized users.

✉ Andrzej A. Romaniuk
Andrzej.Romaniuk@ed.ac.uk

¹ School of History, Classics and Archaeology, University of Edinburgh, Edinburgh EH8 9AG, UK

² Department of Natural Sciences, National Museums Scotland, Edinburgh EH1 1JF, UK

³ School of Geosciences, University of Edinburgh, Edinburgh EH9 3FE, UK

⁴ Oxford University Museum of Natural History, Parks Road, Oxford OX1 3PW, UK

⁵ School of Natural Sciences, University of Manchester, Manchester M1 7DN, UK

⁶ School of Biological Sciences, University of Edinburgh, Edinburgh EH9 3FL, UK

⁷ Department of Collections Services, National Museums Scotland, Edinburgh EH1 1JF, UK

⁸ Skara Brae Publication Project, 509 King Street, Aberdeen AB24 3BT, UK

⁹ Department of Scottish History and Archaeology, National Museums Scotland, Edinburgh EH1 1JF, UK

Introduction

A serious concern when using finite remains to study the past is the destructive nature of many widely adopted methods. It is an especially serious concern in the case of archaeological remains, which are at best a finite resource and often unique (Maschner and Chippindale 2005; Renfrew and Bahn 2012; Frank et al. 2015). Coprolites are a prime example of this problem. Beyond examination of their external appearance and the identification of visible parts of inclusions, the predominant method used to analyse coprolites involves dissection, usually after dissolving (“rehydrating”) the coprolite matrix in a specific solution (Callen 1963), or dry-pulverizing its contents (Heizer 1963), in order to isolate and visually identify any inclusions. However, such approaches narrow the retrievable data strictly to the inclusions and preclude further examination, for example of the internal arrangement of the coprolite content or its chemical composition. Moreover, it precludes the further assessment of those finds in the future with other methods. On archaeological sites where coprolitic finds are relatively common, this problem can be mitigated, for example by utilising subsampling and leaving some coprolites or parts of them for future research. However, many sites provide only a sparse number of coprolites, often as singular finds, and the potential loss of information is too important for a dissection method to be applied.

Because of these drawbacks, in recent decades, there has been a surge in publications exploring potential non-destructive approaches towards archaeological material (e.g. Biró 2005; Borgwardt and Wells 2017). In the case of coprolites, X-ray computed tomography (μ CT) scanning has been utilised for the past two decades to avoid destructive analysis, facilitate replicability and create raw data for future research. Initially used only to generate 2-dimensional cross-sectional data (e.g. Farlow et al. 2010), it has more recently been combined with 3-dimensional (3D) digital imaging techniques for more comprehensive analysis of content and structure (Milàn et al. 2012a, b; Bravo-Cuevas et al. 2017; Wang et al. 2018). This has permitted identification of the coprolite depositor as well as its prey and other food items. Meanwhile, in destructive sampling, one can see a trend towards standardisation of sampling protocols and reduction of sample numbers, which is important to allow replication and therefore reproducibility, and to leave material for analysis with subsequently developed techniques (see Wood and Wilmshurst 2016). Multiple approaches are rarely combined in the study of coprolites; researchers often prefer to use one specific method, and even if this does not destroy a sample, it constrains the diversity of data obtained.

A number of coprolites were found during the excavations of the Neolithic settlement of Skara Brae (Orkney, UK) in 1972–3 (Clarke 1976a, 1976b) and in 1977 (Clarke DV and Shepherd AN *pers. comm.*). The majority of intact coprolites,

alongside many heavily fragmented finds, were retrieved from the settlement core (Trench I). The settlement periphery (Trench II) and off-site Trench III provided only a few finds, in each case confined to a single context. Assuming domestic dogs, *Canis familiaris*, as likely depositors, a parasitological study by Hopkins (Hopkins *J pers. comm.*) examined 58 samples in search of transmission stages of parasites. While the parasitological results were negative, “rehydration” of the coprolites revealed that most contained large numbers of bone fragments. Alongside the general absence of plant material other than microscopic pollen (Clarke DV and Shepherd AN *pers. comm.*), this supports the interpretation that they were deposited by dogs. However, among rehydrated material, eleven samples showed solution colours more similar to ones obtainable from human coprolites, raising the question of whether humans were also responsible for the creation of Skara Brae coprolitic material.

The study herein was designed to provide the maximum data from a series of the available finds, while limiting direct physical impact, to enable their re-examination in the future. The objectives were to identify depositor species and provide data about the depositors’ diet. In contrast to other studies, which generally rely on a single approach, four distinct methods were employed: (1) traditional visual examination; (2) scanning electron microscopy (SEM); (3) high-resolution X-ray micro computed tomography (μ CT); (4) lipid and protein analysis via mass spectrometry. Only the last of these methods required any invasive and destructive measures, in the form of partial coprolite dissection and drilling of several coprolite specimens to obtain samples for analysis.

The study is a part of a bigger research effort of multiple research groups from different research institutions to provide a comprehensive overview of the Skara Brae site and life of its inhabitants during the Orcadian Neolithic period (Clarke and Shepherd *in prep.*).

Materials and methods

As the Skara Brae assemblages contained predominantly heavily fragmented coprolites, only contexts containing intact finds or fragments with identifiable inclusions visible on the surface were selected for this study. Samples from 13 contexts, along with any related bone fragments, were selected for the first stage of analysis (Table 1). Materials from the contexts had been retrieved by sieving with a standard 3-cm mesh. The first nine contexts, containing most of the intact coprolites, represented the second phase of occupation of the main settlement at Skara Brae, dating from around mid-twenty-eighth to mid-twenty-fifth century cal BCE (Sheridan et al. 2013; Shepherd 2016; Bayliss et al. 2017), and corresponding to the bulk of the occupational remains currently visible on the site. In contrast, earlier phases contained far

Table 1 Sampled contexts, including phasing and presence of canid bones (Clarke DV and Shepherd A pers.comm.), and material selected from them for specific methods. Weight (g), intact coprolites with > 75% surface/content present, partial coprolites with 25–75% surface/content present and coprolite fragments with less than 25% surface/content present. Specific methods include computed tomography (CT), protein (Proteins) and lipid (Lipids) analysis, and scanning electron microscopy (SEM)

Context	General context data				Sampled material				Specific methods selection
	Phase	Dog bones present?	Fox bones present?	Amount	Weight	Intact	Partial	Fragm.	
102	2	Yes	No	Whole	9.89	1	2	4	CT: Selected coprolite fragments (20, 7.01 g) SEM: 2 samples Proteins: 3 coprolite fragments
110	2	Yes	No	Sampled	38.39	2	6	39	
170	2	Yes	No	Whole	37.86	7	4	1	CT: Single intact coprolite (6.48 g)
113	2	No	No	Sampled	55.27	5	5	12	CT: Single intact coprolite (14.76 g, after dissection: 6.92 g) Proteins: 10 bone fragments (1.07 g) 1 surface sample
122	2	No	No	Whole	7.17	1	0	0	Lipids: 4 coprolite content samples (1.37 g) CT: Single intact coprolite (7.17 g)
126	2	Yes	No	Sampled	11.07	0	0	34	CT: Selected coprolite fragments (20, 7.71 g) Proteins: 3 coprolite fragments
132	2	No	No	Sampled	6.02	0	0	11	Single intact coprolite (7.83 g) Proteins: 1 surface sample Proteins: 2 coprolite fragments
132.2	2	No	No	Whole	20.36	1	1	54	
134	2	Yes	No	Sampled	38.21	2	18	30	
139	Int.	No	No	Sampled	18.71	3	2	3	
142	1	No	No	Whole	4.50	0	0	6	Single intact coprolite (7.83 g) Proteins: 1 surface sample Proteins: 2 coprolite fragments
157	0	No	Yes	Whole	42.56	0	0	102	
213	1	Yes	Yes	Sampled	102.34	8	13	31	

fewer finds and the remaining four contexts represented the rest of the site stratigraphy (intermediate phase: 139, phase 1: 142, 213; phase 0: 157; details in Shepherd 2016).

The first stage of the research consisted of visual examination of the selected coprolites and associated bone fragments, and further subsampling for subsequent μ CT, SEM and proteomics analysis. Bone or teeth inclusions visible on a coprolite's surface, as well as bone remains with coprolite matrix remains on them, were assessed visually and identification of skeletal element and species was attempted. Vertebrate skeletal material in the National Museums Scotland (NMS) collections was utilised as a source of comparative references for identification, alongside widely used identification books for large (Schmid 1972) and small (Lawrence and Brown 1973; Hillson 2005) mammals. References for taphonomic changes were also used (Andrews 1990; Fernández-Jalvo and Andrews 2016). Intact coprolites and unique finds were photographed and, where advantageous, multiple photo stacking utilised. Following visual analysis, four intact coprolites between 3 and 5 cm in length from contexts 113, 170, 122 and 139, and two sets of fragmented coprolites from contexts 110 and 126, were selected for μ CT scanning.

X-ray micro-computed tomographic data on the internal structure of the intact coprolites were obtained at the University of Edinburgh School of Geosciences Experimental Geoscience Facility. Their in-house, custom-built μ CT system comprises a Feinfocus 10–160 kV dual transmission/reflection source, MICOS UPR-160-AIR ultra-high precision air bearing table, PerkinElmer XRD0822 amorphous silicon X-ray flat panel detector and terbium-doped gadolinium oxysulfide scintillator. Data were acquired using in-house software, reconstructed using filtered back projection in Octopus 8.9 software, and then segmented and visualised using Mimics 19.0. The scan resolution for the larger coprolites was 64 μ m per voxel, and the smaller fragments 26 μ m. Three-dimensional digital reconstructions of the coprolites and their contents were generated to permit analysis of their spatial orientation. Identification of inclusions was also attempted using these reconstructions, as in the initial observation.

The largest intact coprolite, from context 113, was partially dissected to obtain samples for further proteomics analysis. Dissection included 7.8 g of the coprolite, approximately 53% of its whole weight, and provided 10 bone fragments ranging in weight from 0.02 to 0.24 g; these bone fragments were analysed by collagen peptide mass fingerprinting (also called ZooMS: Zooarchaeology by Mass Spectrometry; Buckley et al. 2009). An additional set of 10 samples of coprolite matrix were also taken by drilling two intact coprolites (from contexts 113 and 139) and powdering coprolite fragments from three contexts (see Table 1). A standard proteomic method was used for all 20 samples, in which 6 M GuHCl was added to 100 mg sample and incubated at 4 °C overnight.

Proteins were then ultrafiltered using 10 kDa Vivaspin (UK) ultrafiltration units, into 50 mM ammonium bicarbonate, and the retentate reduced and alkylated with dithiothreitol and iodoacetamide respectively following previously used methods (Wadsworth et al. 2017), prior to tryptic digestion overnight at 37 °C. The digests were then acidified to 0.1% trifluoroacetic acid (TFA), zip tipped with OMIX C18 pipette tips into 50% acetonitrile/0.1% TFA solutions and dried to completion. After re-suspension in 5% acetonitrile/0.1% formic acid, the digests were analysed by LC-Orbitrap Elite mass spectrometry following Buckley et al. (2015). Searches were carried out using Mascot (Perkins et al. 1999) against the SwissProt database containing 556,568 sequences with fixed carbamidomethyl C modifications and variable oxidations of P, K and M, as well as allowance for deamidations of N and Q residues. Only proteins with 2 or more peptides above the homology threshold were considered. ZooMS analyses on the 10 bone fragments were carried out following van der Sluis et al. (2014), in which the 0.6 M hydrochloric acid-soluble fraction following overnight decalcification was ultrafiltered into 50 mM ammonium bicarbonate and digested with sequencing grade trypsin overnight at 37 °C. The samples were then zip-tipped into 10% and 50% acetonitrile fractions, dried completely and resuspended then spotted onto a stainless steel matrix assisted laser desorption ionization (MALDI) target plate. The fingerprints were acquired using a Bruker Ultraflex II MALDI Time of Flight mass spectrometer collecting over the m/z range of 700–3,700 with up to 2,000 laser acquisitions and compared to reference spectra biomarkers presented by Buckley et al. (2017).

An additional four samples of internal coprolite matrix > 0.3 g were taken from different parts of the coprolite for potential taxonomic identification via lipid analysis (e.g. Harraut et al. 2019). The lipids were extracted following established methods (Evershed et al. 1990; Charters et al. 1993) and to maximize the amount available for analysis, three of the coprolite samples were combined (0.74 g in total). The sample was extracted by ultrasonication, after the addition of an internal standard (20 μ g of tetracosane- d_{50}), with a 10-mL chloroform-methanol mixture (2:1 v/v) and the supernatant liquid was collected after centrifugation. The extraction steps were repeated three times, and the combined total lipid extract (TLE) obtained was evaporated using a rotary evaporator and redissolved in 3 ml of chloroform-methanol mixture. An aliquot (1 ml) of the TLE was taken, dried under nitrogen and 2 ml of 5% methanolic sodium hydroxide solution (9:1 MeOH: H₂O) was added. After heating at 70 °C for 1 h, with regular mixing, the mixture was allowed to cool, acidified to pH ~ 3 with 1 M HCl and the organic fraction was extracted using hexane (2 ml, three times). This fraction was dried under nitrogen, 100 μ L of a BF₃-CH₃OH complex was added and heated at 75 °C for 1 h. The solution was cooled, 2 mL of dichloromethane washed double distilled water was added,

and the organic fraction was extracted using chloroform (1 mL, three times), dried under nitrogen and frozen until GC-MS analysis. For GC-MS analysis, the residue was dissolved in 100 μ L of hexane. A second aliquot (1 ml) of the TLE was dried under nitrogen, 50 μ L of N,O-Bis(trimethylsilyl)trifluoroacetamide (BSFTA) was added and the mixture was heated at 60 °C (1 h). The excess BSFTA was evaporated to dryness under nitrogen, and the residue was dissolved in 100 μ L of hexane and immediately analysed by GC-MS.

The samples were analysed using an Agilent 7890A gas chromatograph fitted with a Zebtron ZB-5MS capillary column (30 m, 0.25 mm i.d., 0.25- μ m film thickness) coupled to an Agilent 5975C MSD single quadrupole mass spectrometer operated in electron ionization (EI) mode in scan/SIM mode (scanning a range of m/z 50–650 at 1 scan s^{-1} with a 4-min solvent delay; ionization energy 70 eV) and Agilent 7683 autosampler. The injector port temperatures were set at 280 °C, the heated interface at 280 °C, the EI source at 230 °C and the MS quadrupole at 150 °C. Helium was used as the carrier gas with a flow rate of 1 ml/minute and the samples were introduced in the pulsed splitless injection mode. The oven was programmed from 50 to 130 °C at 20 °C min^{-1} , followed by a rate of 6 °C/min to 310 °C and held at this temperature for 15 min. Compounds were identified by comparison with spectra from the literature.

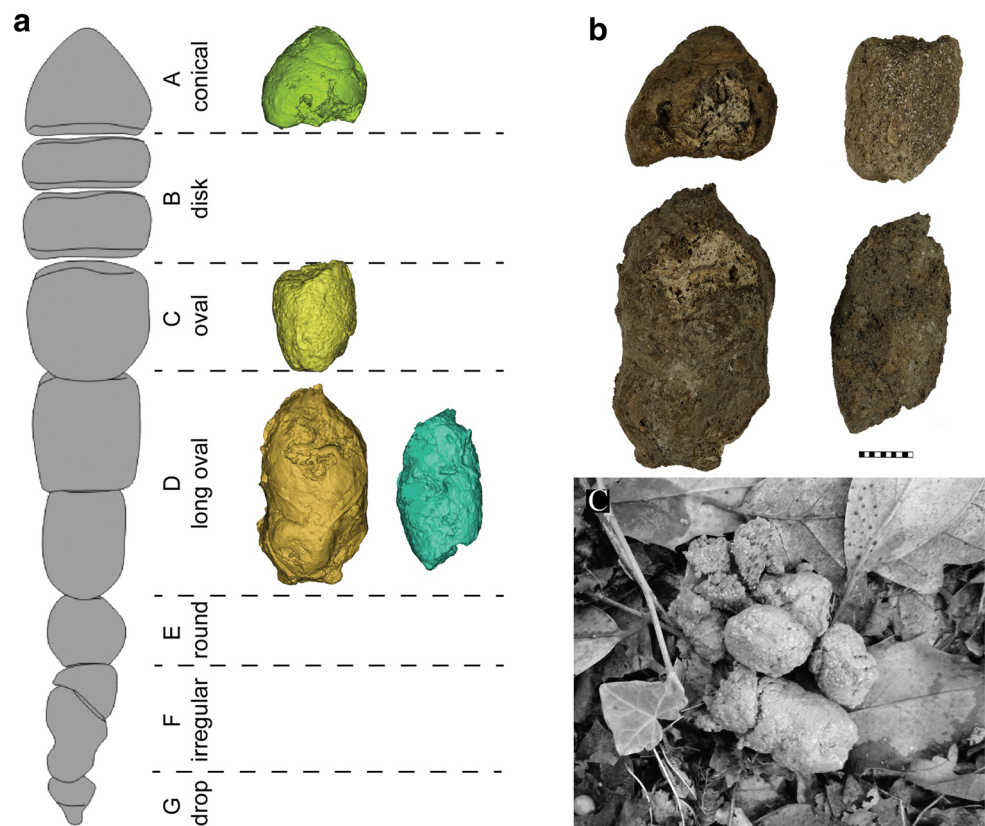
Micromammal inclusions occasionally retrieved from fragmentary coprolites during drilling for samples were assessed using a MX 2500 CamScan scanning electron microscope working with a backscattered detector (SEM-BSC) in Envac mode (50 Pa). The samples were observed without any surface preparation at the working distance of 20 mm using 20 kV accelerating voltage. The scans were used to examine the effects of digestion on bone and tooth surfaces and its impact on the overall preservation of elements, similarly to the examples in available literature (Andrews 1990; Fernández-Jalvo and Andrews 2016).

All coprolite materials (apart from fragments completely powdered for proteomic analysis) remain accessible in the research collections of the National Museums of Scotland and all datasets generated during this research are available online.

Results

The external shape of the coprolites from Skara Brae correlates with mid-size canid species (see Fig. 1). An external typology of carnivoran faeces was developed by Diedrich (2012, Figs. 4 and 6) based on modern African spotted hyaenas (*Crocuta crocuta crocuta*, Erxleben, 1777), in order to study coprological remains from European sites attributed to *Crocuta crocuta spelaea* (Goldfuss, 1823). Applying

Fig. 1 **a** Comparison of four intact coprolites to the line of hyaena droppings (on the left, after Diedrich 2012); **b** Digital photographs of selected coprolites (scale bar 10 mm); **c** Modern example of dog faeces (below). Images copyright National Museums Scotland



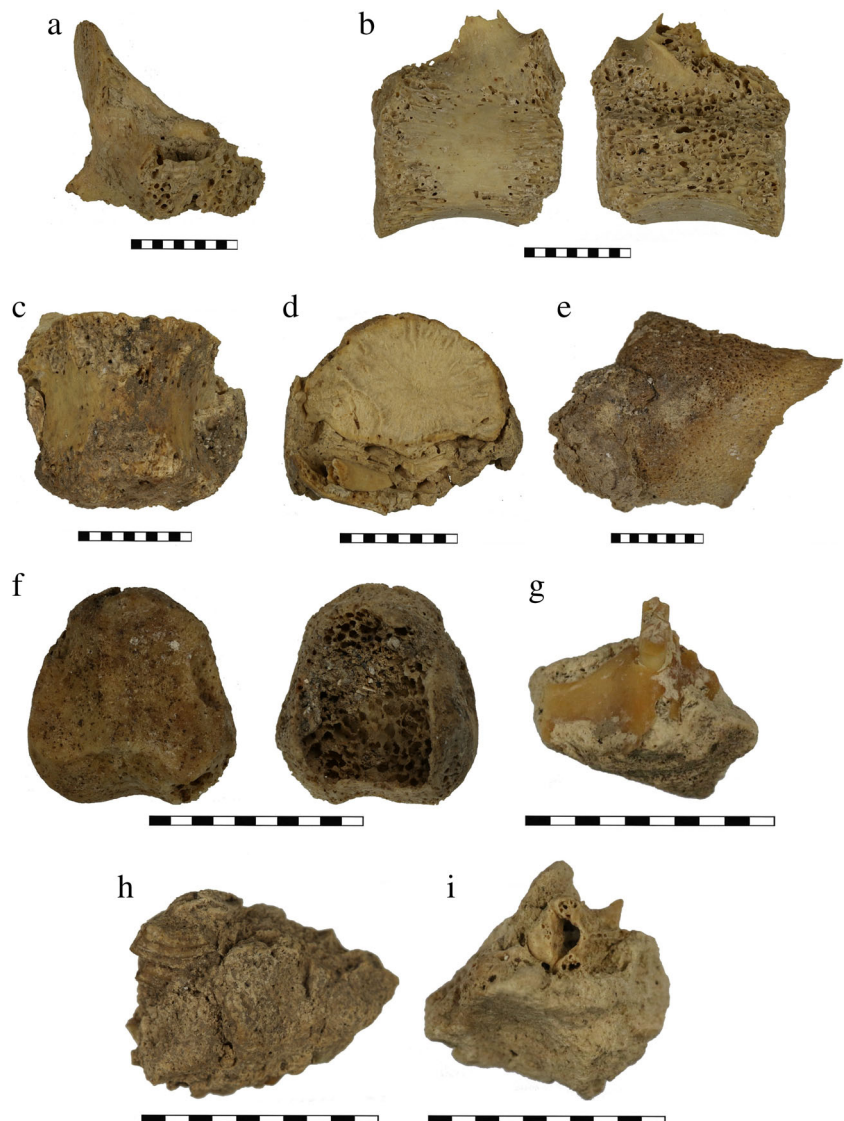
Diedrich's hyaena typology, the larger Skara Brae coprolites that were sampled for μ CT are identified as form A (conical, beginning of the dropping line; context 122), C (oval, mid-dropping line; context 139) and D (long-oval; context 110 and 113) (Fig. 1a). Smaller coprolites resembled types E (round), F (irregular) and G (so-called drop, fragmented end of a complete dropping).

Inclusions exposed on coprolite surfaces were almost exclusively fragmented bone and teeth. The majority of bone inclusions were either small fragments of cancellous (trabecular or spongy) bone, sometimes partially covered by remains of the cortical bone layer. This is similar to those reported from Links of Noltland (Carrot 2011) as well as in previous Skara Brae research (Hopkins J pers. comm.). Bone fragments composed only of cortical bone were also common. Larger and more complete skeletal remains were rarely present and only accessible within fragmented coprolites retrieved from

contexts 170, 113, 126, 132.2 and 139. Evidence for plant remains were scarce. Only one possible example was identified among the intact coprolites included in the μ CT analysis. This comprised a hollow, cuboid depression in the outer shell of a coprolite from context 122, with its surface covered in regular linear impressions, akin to plant fibres (Online Resource 1). Inorganic inclusions were occasionally present in the form of fine gravel or lumps of sand, covering up to 10% of the coprolite surface in the case of the intact coprolite from context 139.

Identification of larger remains attributed to ungulates was hampered by the degree of fragmentation, with only a few morphological features remaining intact. Four fragments of ungulate thoracic vertebra were retrieved from contexts 113 and 126, including a pedicle fragment and anterior vertebral body with unfused epiphyses (Fig. 2a, b) as well as a matching vertebral body and epiphyseal plate encased in two separate

Fig. 2 Identified skeletal fragments found within Skara Brae coprolite assemblages. Contexts are 113 (a, b), 126 (c, d, f), 170 (e), 110 (g, i) and 139 (h). In the case of B and F, two perspectives were included for the sake of clarity. All scale bars 10 mm. Images copyright National Museums Scotland



coprolite fragments (Fig. 2c, d). In addition, two distal limb fragments were found in contexts 170 and 126 (Fig. 2e, f): the distal and unfused part of an ungulate metapodial shaft, and the proximal end of an intermediate phalanx of a sheep. Additionally, context 126 contained three bone fragments, two of which could be identified as the epiphysis of a long bone and the shaft of a rib.

Identification of rodent remains was more straightforward due to the presence of relatively intact teeth and bones. Molar teeth from voles were found in four coprolite fragments, three from context 110 and one from context 139. In context 110, two teeth were still located in the sockets of an almost complete maxillary bone (Fig. 2g), and a third tooth was found separately. In context 139, a complete molar tooth row was present in anatomical sequence within the coprolite matrix, but without any bone remaining (Fig. 2h). Two complete vole vertebrae were found in context 110 (Fig. 2i), and one group of vole metapodials were found in context 126.

The majority of identified inclusions exhibited taphonomic changes on their surface related to bone breakage during ingestion or digestion (Fig. 3). Alterations to the ungulate vertebrae suggest a depositor species trying to bite through, or bite off, their parts. This was especially clear in the case of context 113, where a vertebral body was fragmented roughly along the sagittal plane (Fig. 2b), with the resulting exposure of trabecular bone forming a surprisingly straight layer, even after digestion. Signs of bone fragmentation due to chewing could also be seen on a proximal phalanx from context 126 (Fig. 2f), of which the shaft was also crushed. On the complete

vertebral body from context 126, anterior parts of superior and inferior ridges appeared to have been chewed off in a manner similar to one from context 113. Another taphonomic change visible on the bone surface is heavy digestive corrosion. Digestion appears to have penetrated the cortical layer of bone, creating a wavy cracking pattern as well as thinning it considerably and partially exposing the trabecular structure beneath. In some cases, such as the metapodial fragment from context 170, cortical bone was removed to the point of revealing trabeculae on the whole surface.

SEM micrographs of micromammal bones also revealed digestion characteristic of diurnal raptors or carnivorous mammals (Fig. 4a–d; see Andrews 1990; Fernández-Jalvo and Andrews 2016). In contrast to the larger inclusions, these bones were not broken, thus permitting the study of digestion marks without the obstruction caused by fragmentation. Vole molars were altered considerably, with enamel on the salient edges heavily thinned or chipped away and cementum irregularly fragmented between them (Fig. 4a). Exposed dentine was also partially eroded, creating a surface sloping towards the eroded enamel. Similarly to the larger remains, the surface of the micromammal bones exhibited either wavy cracking (a maxilla, Fig. 4b), or thinning and exposure of trabeculae (Fig. 4c, d).

The μ CT data provided more information on bone inclusions present within the sample. All four intact coprolites predominantly contained small fragments of cancellous (trabecular or spongy) bone densely packed within the matrix (Fig. 5). Only four bone fragments were > 2 cm (largest 29.37 mm),

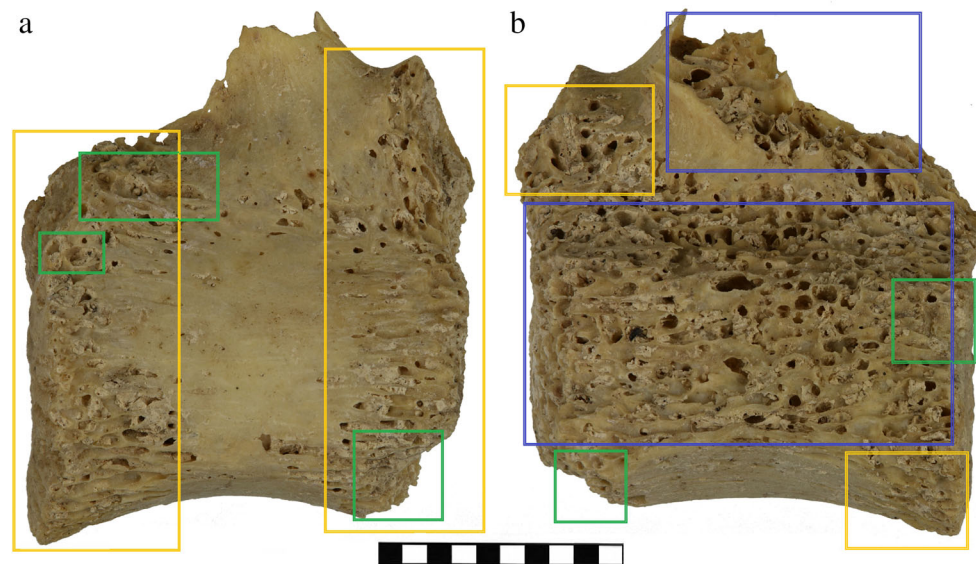
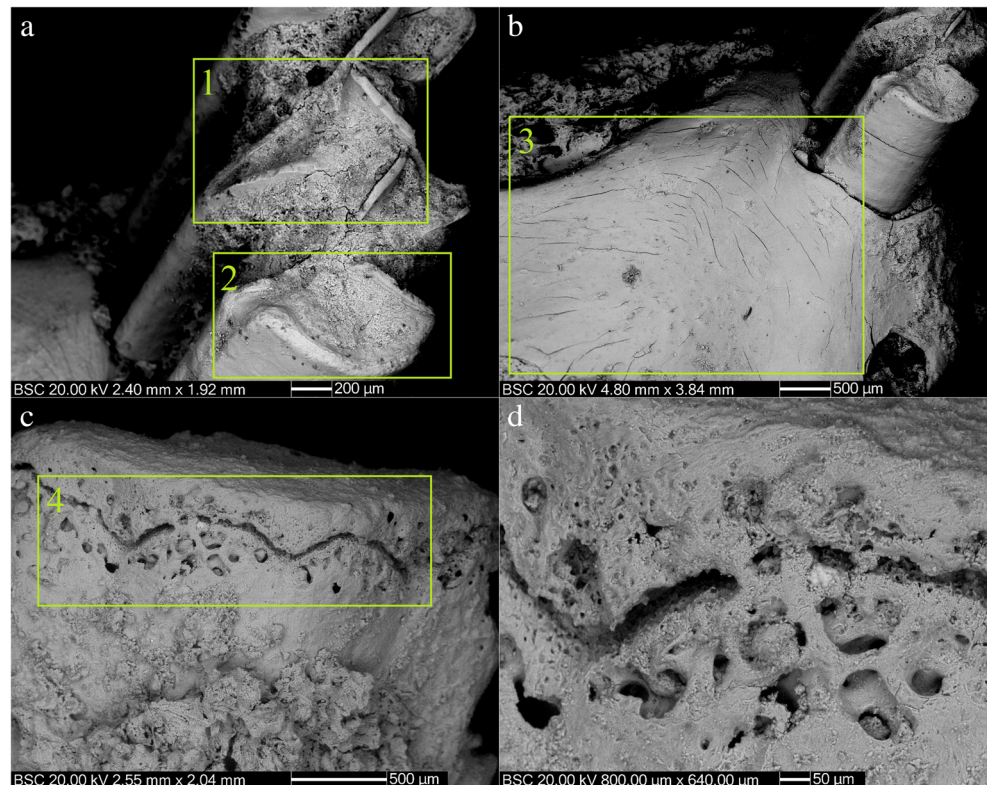


Fig. 3 Example of a bone with various taphonomic marks present (vertebra from context 113, see Fig. 2b). Several minor tooth marks (highlighted in green) are present on both cranial and caudal side of the vertebral body, suggesting that the vertebra was at some point chewed through, leaving half of vertebral body and most of vertebral arch missing (highlighted in blue). Remaining surfaces, especially around ridges of caudal and cranial end, were further altered by digestion, leaving cortical

(surface) layer of the bone thinner or even removed, leaving trabecular (spongy) bone structure inside clearly visible. Chewing of the ridges itself could also help in digestive acids to penetrate the bone to a degree currently visible. See Fernández-Jalvo and Andrews (2016, Fig. A.152, 355 & 816) for comparisons. Scale bar 10 mm. Images copyright National Museums Scotland

Fig. 4 SEM micrographs of two micromammal finds retrieved from context 110 assemblage: Orkney vole maxilla (**a, b**) and rodent (vole?) vertebral body (**c, d**). Areas in (**a**) show chipping (1) or sloping digestion (2) of molar enamel, with exposed dentine beneath also showing sloping loss towards enamel outline. Area 3 in (**b**) in turn shows digestive changes on bone tissue, in a form of a wavy cracking on even cortical surface. In case of area 4 in (**c**) (seen in detail in **d**), cortical layer erosion alongside vertebral epiphyseal line can be seen. Thinning of the bone in several cases leads to the creation of large perforations, exposing trabecula beneath. Epiphyseal line itself may be visible only due to erosion. Images copyright National Museums Scotland

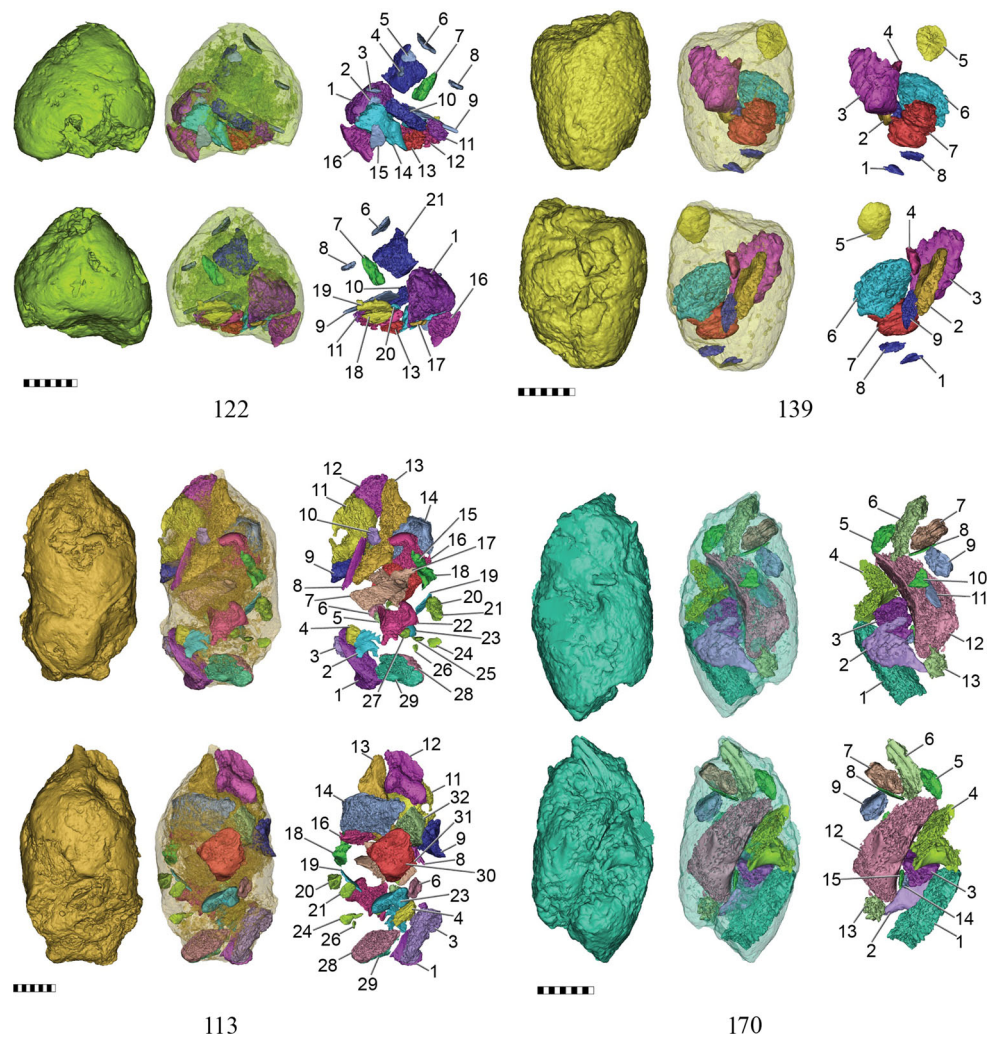


which is similar to the size of finds identified from visual assessment. Of the 73 fragments within the coprolites, 30 fragments ranged between 1 and 2 cm in length, and the remaining 43 were < 1 cm in length. The percentage of bone in the coprolite, by volume, ranged from 11.56% (coprolite from context 139) to 21.65% (coprolite from context 170). The number of bone fragments within each coprolite correlated with its overall size, the largest coprolite (113) containing 32 fragments, the smallest (139) containing only nine and the intermediate-sized coprolites containing 21 (122) and 15 (170). The coefficient of determination between the length and width of the inclusions was relatively high, with a combined r^2 for all four coprolites of 0.74 (correlation = 0.86, for $df = 76$ significant over 0.2). For three coprolites, the r^2 was higher (0.85–0.89), whereas for the coprolite from context 113, it was only 0.61, possibly due to the length to width ratio of the largest fragment within it (no. 13, see Fig. 5 and Online Resource 3), which differed from the rest of the fragments present. Bone was most likely crushed into fragments of similar size as a result of mastication or later digestion. Larger bone fragments were located deeper within the coprolite matrix. The mean depth of the 10 largest bone fragments was 4.84 mm, as opposed to 2.99 mm for all of the other fragments studied. This is best seen in coprolites from contexts 170 ($r^2 = 0.70$ for length/depth and $r^2 = 0.84$ for width/depth) and 139 ($r^2 = 0.66$ and $r^2 = 0.78$). In the case of a coprolite from context 122, the results ($r^2 = 0.31$, $r^2 = 0.33$) were skewed towards the largest fragment (no. 2, see Fig. 5) and rose significantly when it was omitted from the sample pool ($r^2 = 0.57$, $r^2 = 0.81$). In contrast, the coefficients for

the coprolite from context 113 ($r^2 = 0.30$, $r^2 = 0.41$) were generally low and the removal of outliers did not change the outcome significantly. Weight data obtained from 10 bone fragments retrieved from an intact coprolite from context 113 showed the highest coefficient with width ($r^2 = 0.88$), with the other two measurements providing moderate values ($r^2 = 0.46$ for length, $r^2 = 0.43$ for depth).

Only one bone, fragment 23 from context 113, was morphologically intact within the coprolites (Fig. 5c). It was located using the digital 3D reconstructions and later dissection. Considering its size (length of ~ 1 cm), shape and the location of an articular surface on only one side of the bone, it is identified as a carpal, most likely a pisiform from a small to medium-sized ungulate. The most similar bone among the reference material was the left pisiform of a domestic sheep, which is of approximately the same length, shape and facet orientation. The only morphological difference in fragment 23 was a depression visible in the 3D digital reconstruction, running from the end of the articular facets to a narrow ridge on top of the bone, and possibly representing loss of cortical bone. Once retrieved during the dissection (Online Resource 2), the assessment based on the digital reconstruction was confirmed, both with regard to the identification as a pisiform and the presence of an area with trabecular bone exposed. The perforation of the cortical bone near the articular facet seems to have been created by chewing, and the surrounding areas of exposed trabecula the result of the subsequent digestive processes.

Fig. 5 Digital reconstructions of intact coprolites from microCT data. Two perspectives are shown for each coprolite, including external surface and internal composition of bone fragments, and inclusion numbers (for more data about specific inclusions see Online Resource 3. All scale bars 10 mm. Images copyright National Museums Scotland



Other inclusions from the coprolite from context 113 could not easily be identified visually. From the digital reconstructions, it is possible to infer high levels of bone fragmentation, and inclusions with trabecular bone exposed were reminiscent of epiphyses of limb bones, especially metapodials or phalanges. But, the identity of other bone fragments, notably the thin elements reminiscent of flat bones rather than long ones, could not be established. Fragments obtained during dissection showed extreme alteration caused by digestion, with many exposed trabeculae visible through the mostly digested cortical layer. Although exact anatomical or taxonomical provenance could not be established, the most likely source was smaller distal limb bones, possibly of an ungulate.

Remains within the other large coprolites were less informative, but suggest the same interpretation as for the coprolite from context 113. The coprolite from context 170 contained fragment 12, a large chunk of trabecular bone covered on one side by a thin and slightly concave cortical bone layer. Considering its shape and size, it could be a part of a proximal phalange or similar skeletal element. Similarly, the coprolite

from context 139 contained fragment 5, a disc-like structure reminiscent of a small (< 1 cm in diameter) epiphyseal plate. One side of fragment 5 was smooth and slightly convex, the other was covered in billowing formations not uncommon on epiphyseal surfaces. Among the two sets of fragmented coprolites, inclusions could only be found in those from context 126, and these were identified as the proximal tibial epiphysis and a segment of a sacrum from a rodent.

While biochemical analysis of coprolite matrix did not return conclusive results, proteomics on bone inclusions from a dissected coprolite provided additional information about species provenance (Table 2). Proteomic analysis of the coprolite matrix samples from multiple coprolites yielded very few informative peptides, with some appearing devoid of peptide matches (samples 17 and 19) and others either containing single peptides per protein ‘match’ or multiple from keratins, especially human. Such proteins could derive from various forms of contamination. Lipid analysis of the coprolite matrix also did not provide depositor or prey identification. The first fraction (Aliquot 1) was dominated by a homologous series of

Table 2 Details of samples extracted from coprolites through dissection (bone fragment and matrix) and drilling (matrix), showing most likely species based on identified proteins/lipids. * indicates likely contaminations. Test samples excluded

Sample type	Context	Sample no.	Bone fr. No.	Weight (g)	Result
Bone fragment (dissection)	113	1	1	0.14	Sheep (collagen)
Bone fragment (dissection)	113	2	3	0.13	—/—
Bone fragment (dissection)	113	3	6	0.02	—/—
Bone fragment (dissection)	113	4	18	0.03	—/—
Bone fragment (dissection)	113	5	22	0.22	—/—
Bone fragment (dissection)	113	6	23	0.05	—/—
Bone fragment (dissection)	113	7	24	0.01	—/—
Bone fragment (dissection)	113	8	28	0.06	—/—
Bone fragment (dissection)	113	9	29	0.18	—/—
Bone fragment (dissection)	113	10	30	0.24	—/—
Matrix (dissection)	113	A	—	0.33	Unknown (saturated & unsaturated fatty acids & alcohols, unknown sterols, plastic derivatives*)
Matrix (dissection)	113	B	—	0.36	—/—
Matrix (dissection)	113	C	—	0.33	—/—
Matrix (dissection)	113	D	—	0.36	—/—
Matrix (drilling)	110	11	—	—	Human* (keratin)
Matrix (drilling)	110	12	—	—	—/—
Matrix (drilling)	110	13	—	—	Human* (multiple skin proteins)
Matrix (drilling)	113	14	—	—	Human* (keratin)
Matrix (drilling)	126	15	—	—	—/—
Matrix (drilling)	126	16	—	—	—/—
Matrix (drilling)	126	17	—	—	? (trypsin only)
Matrix (drilling)	139	18	—	—	Human* (keratin)
Matrix (drilling)	142	19	—	—	? (trypsin only)
Matrix (drilling)	142	20	—	—	Human* (keratin)

C₁₂–C₂₈ *n*-alkanoic acids, with the C₁₆ (hexadecanoic acid) and C₁₈ (octadecanoic acid) member being the most abundant. The high molecular weight (HMW) *n*-alkanoic acids (>C₂₀) showed a clear even-over-odd carbon number predominance in line with a plant derived origin. Also present were a series of the monounsaturated C₁₂–C₁₈ alkanolic acids. The second fraction (Aliquot 2) was dominated by homologous series of C₁₀–C₃₂ *n*-alkanols, with the C₂₆ member being the most abundant. The HMW *n*-alkanols showed a clear even-over-odd carbon number predominance in line with a plant derived origin. Also present were some contaminants, including the alkyl phthalates and alkyl phenol derivatives, as well as minor amounts of cholesterol and cholestanol. However, in contrast to previous studies, no faecal stanols, such as coprostanol, epicoprostanol, 24-ethylcoprostanol or 24-ethylepicoprostanol, could be identified (Bull et al. 2002; Gill et al. 2009; Harrault et al. 2019). In turn, collagen fingerprinting of the bone samples showed a strong signal for the presence of sheep collagen. Moreover, all bone samples, including fragment 23 from context 113 (the morphologically

intact bone described above), returned the same identification. It is likely that most bones within the coprolite came not only from the same species, but also the same animal.

The μ CT scan data revealed differences between the inner and outer layers of three of the four intact coprolites. A mineralised outer layer, denser than the coprolitic matrix and of similar greyscale values to the dense cortical bone content, was especially evident in the coprolite from context 122. Although one coprolite from 110 also exhibited such a layer, it did not encase the entire contents, notably being absent where the bone content was visible at the surface or the coprolite itself was apparently eroded. The coprolite from context 113 also had a mineralised outer layer, but it was thinner and less visible in the μ CT data. The coprolite from context 139 did not show any outer layer mineralisation.

CT and visual data from the Skara Brae coprolites were similar to previous observations of the contents of the faeces of dogs (Payne and Munson 1985), but differed somewhat. In their experiment, a dog was fed parts of specific animals of three different body sizes (the largest being domestic goat,

Capra hircus; intermediate being eastern cottontail rabbit, *Sylvilagus floridanus* and the smallest fox squirrel, *Sciurus niger* and grey squirrel, *S. carolinensis*) and surviving inclusions in faecal matter, as well as uneaten remains, were analysed in a variety of ways. As in the results of that study, the Skara Brae material shows a predominance of small fragments (Table 3), although not to the degree reported by Payne and Munson (80–90%). The Skara Brae material comprised 56% fragments < 1 cm in the four μ CT scanned intact coprolites, and 61% including the scanned smaller fragments and visually assessed material. Payne and Munson also found only a minor part of the assemblage was identifiable, with the size of identifiable fragments related to the size of the prey species to which they belong (1–2 cm for goat, and 0.01–1 cm for lagomorphs and rodents). In the case of Skara Brae however, the situation is more complex due to the presence of species of both sizes within the same coprolite matrix. Only 1.3% of the content of the four intact coprolites could be identified, which is similar to the proportion of goat remains identifiable in Payne and Munson (1985). However, when all the data are considered together, 14.7% of bone inclusions could be

identified to species, more closely resembling the data from smaller species’ ingestion. Among the identified remains, vole bones smaller than 1 cm dominated, followed by far larger ungulate remains, 2–3 cm in diameter. Only two remains were identified within the range of 1–2 cm, leaving a distinct gap between the size of the two ingested species.

Discussion

Although some non-food elements may accidentally be ingested or attached to faeces after deposition, such as gravel or small particulates, the majority of coprolite contents should faithfully represent the diet of the depositor (Hunt et al. 1994). The best known coprolite assemblages are predominantly of canid origin, and have been studied since the nineteenth century (Buckland 1823). More recently, canid coprolites have been examined using μ CT scanning to analyse their internal structure (Bravo-Cuevas et al. 2017; Wang et al. 2018). The internal composition of the four intact coprolites from Skara Brae resembles that of finds examined in Wang et al. (2018),

Table 3 Comparison of greatest length for bone fragments from Skara Brae (intact coprolites only versus all gathered data) with those from coprolites of dogs fed on three mammal species, selected to represent a

range of size classes (Payne and Munson 1985), data presented in size classes (1 cm intervals)

Maximal length	Coprolite fragments from Skara Brae, major finds (CT, 4 major coprolites)				Coprolite fragments from Skara Brae, all finds (visual + CT)			
	Overall	as%	Identified	as%	Overall	as%	Identified	as%
Size class								
4.00–4.99	0	0.00	0		0	0.00	0	
3.00–3.99	0	0.00	0		0	0.00	0	
2.00–2.99	4	5.19	0	0.00	9	7.76	5	29.41
1.00–1.99	30	38.96	1	100.00	36	31.03	2	11.76
To 0.99	43	55.84	0	0.00	71	61.21	10	58.82
Overall	77	–	1	1.30	116	–	17	14.66
Maximal length	<i>Capra</i> remains in dog faeces (Payne and Munson 1985 t.5)				<i>Sylvilagus</i> remains in dog faeces (Payne and Munson 1985 t.5)			
Size class	Overall	as%	Identified	as%	Overall	as%	Identified	as%
4.00–4.99	1	0.01	0	0.00	0	0.00	0	
3.00–3.99	28	0.36	6	5.61	0	0.00	0	
2.00–2.99	221	2.82	33	30.84	4	0.65	1	2.33
1.00–1.99	1127	14.37	64	59.81	44	7.20	4	9.30
To 0.99	6466	82.44	4	3.74	563	92.14	38	88.37
Overall	7843	–	107	1.36	611	–	43	7.04
Maximal length	<i>Sciurus</i> remains in dog faeces (Payne and Munson 1985 t.5)							
Size class	Overall	as%	Identified	as%				
4.00–4.99	0	0.00	0					
3.00–3.99	0	0.00	0					
2.00–2.99	2	0.40	2	1.54				
1.00–1.99	67	13.45	32	24.62				
To 0.99	429	86.14	96	73.85				
Overall	498	–	130	26.10				

attributed to the extinct bear-dog *Borophagus parvus*, with a number of fragmented bones entrapped completely or almost completely within the fossilized faecal matter. However, in contrast to the bear-dog, or unidentified canids in other studies (e.g. Bravo-Cuevas et al. 2017), the Skara Brae dog faeces contain fewer identifiable remains, most being too finely fragmented to permit the recognition of anatomical and taxonomical provenance. Bone inclusions from Skara Brae were also tightly condensed, often with only a small amount of coprolite matrix between the pieces of trabecular bone. These differences may be attributed to *Borophagus parvus* being a bone-crushing canid, with specialisations in dentition and digestion to chew and ingest most of the skeletal structure of their adult prey (Wang et al. 2018). On the other hand, modern wolves (*Canis lupus*) and dogs do not exhibit this specialism, relying on chewing easily modifiable elements, often from younger prey, and often smaller bones and long limb epiphyses (Fosse et al. 2012).

The visual methods and proteomics both confirmed the prey species as being sheep, whose main skeletal elements cannot be ingested whole by dogs. As a result, they are potentially not identifiable when sufficiently fragmented to be swallowed. However, minor skeletal elements, for example phalanges or vertebrae, could be ingested either complete or in fragments that are large enough to be identifiable. Considering that some bones came from immature individuals (as evidenced by the lack of epiphyseal fusion), dogs from Skara Brae were most likely fed by humans; low meat-bearing distal limbs and vertebral spines would have originated from butchery products and meal waste.

The abundance of highly fragmented and digested bones within the Skara Brae coprolites points unmistakably towards a typical carnivorous species fed by humans or actively scavenging human refuse. Such a species is represented at Skara Brae by domestic dogs (Clarke 1976B; Clarke and Sharples 1985; Clarke DV and Shepherd AN pers. comm.). Scattered dog remains were found in multiple contexts from the middle stage of phase 1 until the late stage of phase 2, including the intermediate period between both phases. Many of these remains were isolated teeth, suggesting deposition from natural tooth loss rather than death of the animal.

Although the remains of two other carnivore species were also found in Skara Brae (Clarke DV and Shepherd AN pers. comm.), they are less likely to have deposited the coprolites. Red fox (*Vulpes vulpes*) finds were located in contexts belonging to the earliest two phases (0 and early/middle 1), and these do not correlate with the main bulk of the coprolite finds (phase 2). Their remains mainly comprised long limb bones and innominates, along with a single jaw. This suggests the processing of foxes to obtain their pelts. It is also debateable whether red foxes were living wild on Orkney at that time; foxes were most likely present from the Early Iron age until the Late Norse period (Fairnell and Barrett 2006), two

millennia after the deposition of the Skara Brae remains. However, as for the pine marten (*Martes martes*) remains from the Neolithic Pierowall Quarry on Westray, Orkney, such finds could be a sign of a short-lived local population (Sharples 1984). Evidence for a third carnivore found at Skara Brae was the single find of an otter (*Lutra lutra*) metacarpal. Otters are generally considered to be intrusive at archaeological sites, and produce highly characteristic faeces ('spraint'), which are clearly morphologically different from the Skara Brae coprolitic finds.

The presence of a hard outer coating is considered a typical feature of fossilized carnivore faeces (Bryant 1974). This coating corresponds to the mineralised outer layer present on the Skara Brae coprolites. As first suggested by Bradley (1946), and confirmed by recent studies (Hollocher et al. 2010; Pesquero et al. 2014), calcium phosphate and other bone mineral content in coprolites contributes to their long-term preservation. The only intact Skara Brae coprolite without such a coating still contained bone, but a smaller amount than the other three finds. This appears to confirm the relationship between bone content in the creation of an outer coating. It may also point towards differential diagenetic processes between contexts, although it is currently not known exactly how this may contribute to coprolite preservation and mineral content.

Considering the findings of the visual and μ CT analyses, Neolithic humans, as omnivores, are unlikely to be depositors of the studied coprolites. Human faeces are usually diverse in their contents (containing bones, fibres, seeds, etc.) and the mineralised coating attributable to carnivores does not usually occur on their surface (Callen 1963; Heizer 1963; Bryant 1974; Reinhard and Bryant 1992; Reinhard 2000). However, research on excavated coprolites of possible human origin almost exclusively relies on DNA-based identifications (e.g. Gilbert et al. 2008; Jenkins et al. 2012; Petrigh and Fugassa 2017) or microbiological studies (Cano et al. 2014), with only a marginal interest in bone inclusions. As a consequence, there is a lack of visual and μ CT data on human coprolites to provide a comparative dataset for our analysis. Regular human coprolite deposition would also be unlikely from the contextual perspective. Skara Brae had a form of drainage system which could be used regularly for removing human faeces (Shepherd 2016; Clarke and Sharples 1985), leading to such material being transported outside of the site or gathered as a manure for nearby fields (Clarke and Sharples 1985). The majority of coprolite finds came from deposits behind and between settlement structures, areas more likely to be frequented by animals rather than humans.

The presence of micromammal remains provides evidence of other processes taking place at the site. Orkney vole remains from Skara Brae coprolites are much smaller than the North American pocket gophers (*Pappogeomys/Cratogeomys*) in canid coprolites studied by Bravo-Cuevas

et al. (2017), but show a similar level of preservation, with fragments being easily identifiable anatomically and in many cases also taxonomically. Previous research on the Skara Brae micromammal assemblages found significant concentrations of rodents within the site centre (Trench I) and periphery (Trench II), possibly related to human occupation (Romaniuk et al. 2016). Two likely explanations were that these are the remains produced as a by-product of pest control, or processing of micromammals as a food source. Dogs may have been fed voles in the absence of addition to the routine meal or butchery waste; possibly, they were trained to hunt such animals as a form of pest control, or simply caught and ate them of their own volition. Modern dogs on Orkney are known to hunt rodents, but are rarely reported as eating them (Rose 1975). Micromammal bones are also known to appear in human coprolites (Reinhard and Bryant 1992; Reinhard et al. 2007), but in the case of Skara Brae, the coprolite fragments in which inclusions were found did not differ substantially from the rest of the coprolite assemblage, established in previous paragraphs to resemble canid deposition. However, it is unlikely that deposition by dogs, even over a longer period of time, was responsible for all of the micromammal finds from the excavations at Skara Brae. The micromammal inclusions show severe taphonomic alterations of bone and tooth surfaces characteristic of carnivore digestion, especially the loss of enamel or dentine and the thinning or cracking of bone. Previous analysis of the micromammal skeletal assemblage from Skara Brae (Romaniuk et al. 2016) did not provide such finds. Signs of digestion on the micromammal remains were scarce and did not follow a pattern that has previously been identified as indicative of any mammalian species.

From a methodological perspective, the present study demonstrates the value of a combined approach, successfully limiting destructive analysis while providing more useful data than reliance on a single method alone. From over 392 g of assemblage, only 5.5 g of content was fragmented during the dissection, and only ~ 2.5–3.0 g was destroyed during the proteomics analysis. Enough material remains to replicate this study in the future while X-ray computed tomography ensured non-direct replicability though reinvestigation of the μ CT data. Of equal importance, the combination of methods provided complementary data and further support for the results obtained by individual methods. Anatomical identifications were based on visual examination combined with digital imaging, while taxonomic identifications benefitted from these methods together with proteomics. Taphonomic changes could be assessed visually, using μ CT, and using SEM imaging. The molecular analyses were more indicative of the dietary component rather than the depositor species, contrary to the reported ability to do the latter. Moreover, dissection proved to be the optimal method to obtain

uncontaminated material from coprolites. Drilled material affected a smaller area of coprolites but showed too much contamination by human proteins.

Conclusions

The combination of visual assessment, μ CT scanning with digital reconstruction, scanning electron microscopy and protein/lipid analysis all in one study is presently rare. This approach has proven especially useful in identifying coprolite depositors and providing data about their possible diet. A number of bone fragments embedded on or within the coprolite matrix were investigated and identified as the distal limb bones or vertebrae of an ungulate, possibly sheep. Proteomics confirmed the presence of sheep collagen within bone inclusions sampled during the dissection. Some finds also included relatively complete remains of Orkney voles. Many coprolites had a thick, mineralised outer layer, consistent with a typically carnivorous diet and the ingestion of large quantities of skeletal remains. The majority of finds, including all μ CT scanned intact coprolites, were likely deposited by dogs. As the depositor diet shows consumption of the low meat-bearing elements of domesticated species in the anthropic environment, it is likely that these dogs were routinely fed on the refuse of butchery or meals refuse, or scavenged them. Additional micromammal material could come from occasional catches, either as intentional pest-control measures, or subsistence practices.

X-ray computed tomography proved to be useful for the study of intact coprolites, rather than fragmented remains. Study of proteins was useful for assessing bone inclusions embedded within coprolites, but samples of coprolite matrix itself did not yield significant results. This may indicate the necessity of hard tissues for the preservation of prey proteins, as well as the effect of carnivore digestion in removing traces of depositor proteins. Lipid analysis proved to be more useful in the case of coprolite matrix; however, the method needs to be refined, especially with regard to identification and procedures for avoidance of contamination. This case study highlights the benefits of non-destructive and comparative studies on coprolitic finds from archaeological sites, and provides a template for future research methodology.

Acknowledgements We would like to thank the National Museums of Scotland for access to the Skara Brae remains and vertebrate skeletal reference material. Thanks to Dr Stig Walsh, who (along with EP) co-supervised CW during her dissertation.

Author's contributions The study was conceived by AAR, EP and JSH. Data collection and analyses were performed by AAR (traditional visual analysis), LT (SEM), IB, CW and EP (μ CT scanning and digital reconstruction), MB, BEvD and MPC (proteins & lipids). Figures were compiled by AAR and EP. All authors contributed to the writing of the paper and gave final approval for publication.

Funding AAR was in receipt of a School Doctoral Scholarship from the School of History, Classics and Archaeology, University of Edinburgh. EP was funded by NERC, grant number NE/L002558/1. CW carried out μ CT work as part of her undergraduate final dissertation at the University of Edinburgh, funded by The School of Biological Sciences, University of Edinburgh.

Data availability Available data supporting this paper include Excel data file (Online Resource 3), R script file with short statistical analysis (Online Resource 4), compressed file with X-ray computed tomographic data and files containing coprolite 3D digital reconstructions (Online Resource 5), video showing the internal structure of the intact coprolite from context 113 (Online Resource 6) and two additional figures (Online Resource 1 and 2). All files are available online.

Compliance with ethical standards

Competing interests The authors declare that they have no competing interests.

Open Access This article is licensed under a Creative Commons Attribution 4.0 International License, which permits use, sharing, adaptation, distribution and reproduction in any medium or format, as long as you give appropriate credit to the original author(s) and the source, provide a link to the Creative Commons licence, and indicate if changes were made. The images or other third party material in this article are included in the article's Creative Commons licence, unless indicated otherwise in a credit line to the material. If material is not included in the article's Creative Commons licence and your intended use is not permitted by statutory regulation or exceeds the permitted use, you will need to obtain permission directly from the copyright holder. To view a copy of this licence, visit <http://creativecommons.org/licenses/by/4.0/>.

References

- Andrews P (1990) Owls, caves and fossils. University of Chicago Press, Chicago, IL
- Bayliss A, Marshall P, Richards C, Whittle A (2017) Islands of history: the Late Neolithic timescape of Orkney. *Antiquity* 91(359):1171–1188. <https://doi.org/10.15184/aqy.2017.140>
- Biró K (2005) Non-destructive research in archaeology. *J Radioanal Nucl Chem* 265(2):235–240. <https://doi.org/10.1007/s10967-005-0814-6>
- Borgwardt TC, Wells DP (2017) What non-destructive analysis mean? *Cogent Chem* 3(1):1405767. <https://doi.org/10.1080/23312009.2017.1405767>
- Bradley WH (1946) Coprolites from the Bridger Formation of Wyoming: their composition and microorganisms. *Am J Sci* 244:215–239
- Bravo-Cuevas VM, Morales-García NM, Barrón-Ortiz CR, Theodor JM, Cabral-Perdomo MA (2017) Canid Coprolites from late Pleistocene of Hidalgo, Central Mexico: importance for the Carnivore Record of North America. *Ichnos* 24(4):239–249. <https://doi.org/10.1080/10420940.2016.1270209>
- Bryant VM (1974) Prehistoric diet in Southwest Texas: the Coprolite Evidence. *Am Antiq* 39(3):407–420. <https://doi.org/10.2307/279430>
- Buckland W (1823) *Reliquiae diluvianae: Or, Observations on the organic remains contained in caves, fissures, and diluvial gravel, and on other geological phenomena, attesting the action of an universal deluge*. London. <https://doi.org/10.1017/CBO9780511694820>
- Buckley M, Collins M, Thomas-Oates J, Wilson JC (2009) Species identification by analysis of bone collagen using matrix-assisted laser desorption/ionisation time-of-flight mass spectrometry. *Rapid Communications in Mass Spectrometry* 23: 3843–3854. <https://doi.org/10.1002/rcm.4316>
- Buckley M, Farina RA, Lawless C, Tambusso PS, Varela L, Carlini AA, Powell JE, Martinez JG (2015) Collagen sequence analysis of the extinct giant ground sloths *Lestodon* and *Megatherium*. *PLoS One* 10(11):e0139611. <https://doi.org/10.1371/journal.pone.0139611> eCollection 2015
- Buckley M, Harvey VL, Chamberlain AT (2017) Species identification and decay assessment of Late Pleistocene fragmentary vertebrate remains from Pin Hole Cave (Creswell Crags, UK) using collagen fingerprinting. *Boreas* 46: 402–411. <https://doi.org/10.1111/bor.12225>
- Bull ID, Lockheart MJ, Elhmmali MM, Roberts DJ, Evershed RP (2002) The origin of faeces by means of biomarker detection. *Environ Int* 27(8):647–654
- Callen EO (1963) Diet as Revealed by Coprolites. In: Brothwell D, Higgs E (eds) *Science in Archaeology: a survey of progress and research*. Thames & Hudson, London, pp 235–243
- Cano RJ, Rivera-Perez J, Toranzas GA, Santiago-Rodriguez TM, Narganes-Storde YM, Chanlatte-Baik L, García-Roldán E, Bunkley-Williams L, Massey SE (2014) Paleomicrobiology: Revealing fecal microbiomes of ancient indigenous cultures. *PLoS One* 9(9):E106833. <https://doi.org/10.1371/journal.pone.0106833>
- Carrot J (2011) Assessment of possible coprolites. In: Moore H, Wilson G (eds) *Shifting sands: links of Noltland, Westray: interim report on Neolithic and Bronze Age Excavations 2007-2009*. Historic Scotland, Edinburgh, p 108
- Charters S, Evershed RP, Goad LJ, Leyden A, Blinkhorn PW, Denham V (1993) Quantification and distribution of lipid in archaeological ceramics: implications for sampling potsherds for organic residue analysis and the classification of vessel use. *Archaeometry* 35(2):211–223. <https://doi.org/10.1111/j.1475-4754.1993.tb01036.x>
- Clarke DV (1976a) The Neolithic Village at Skara Brae, Orkney, 1972-73 excavations: an interim report. HMSO, Edinburgh
- Clarke DV (1976b) Excavations at Skara Brae: a summary account. In Burgess CB, Miket R. (ed) *Settlement and economy in the third and second millennium B.C.*. British archaeological Reports 33, Oxford, pp. 233-250
- Clarke DV, Sharples N (1985) Settlements and subsistence in the third millennium B.C. In: Renfrew C (ed) *The Prehistory of Orkney*. Edinburgh University Press, Edinburgh, pp 54–82
- Clarke DV, Shepherd AN (*in prep*) Skara Brae: views of a Neolithic life.
- Diedrich CG (2012) Typology of Ice Age spotted hyena *Crocuta crocuta spelaea* (Goldfuss, 1823) coprolite aggregate pellets from the European Late Pleistocene and their significance at dens and scavenging sites. In: Hunt AP, Milàn J, Lucas SG, Speilmann JA (eds) *Vertebrate Coprolites*, New Mexico Museum of Natural History and Science, Bulletin, vol 57. New Mexico Museum of Natural History & Science, Albuquerque, pp 369–377
- Evershed RP, Heron C, Goad LJ (1990) Analysis of organic residues of archaeological origin by high-temperature gas chromatography and gas chromatography-mass spectrometry. *Analyst* 115:1339–1342. <https://doi.org/10.1039/AN9901501339>
- Fairnell EH, Barrett JH (2006) Fur-bearing species and Scottish islands. *J Archaeol Sci* 34:463–484. <https://doi.org/10.1016/j.jas.2006.09.005>
- Farlow JO, Chin K, Argast A, Poppy S (2010) Coprolites from the Pipe Creek sinkhole (Late Neogene, Grant County, Indiana, U.S.A.). *J Vertebr Paleontol* 30(3):959–969. <https://doi.org/10.2307/40666208>
- Fernández-Jalvo Y, Andrews P (2016) *Atlas of Taphonomic Identifications: 1001+ Images of Fossil and Recent Mammal Bone Modification*. Springer, New York, London

- Fosse P, Selva N, Smietana W, Okarma H, Wajrak A, Fourvel JB, Madelaine S, Esteban-Nadal M, Cáceres I, Yravedra J, Brugal JP, Pruca A, Haynes G (2012) Bone modification by modern wolf (*Canis lupus*): a taphonomic study from their natural feeding places. *J Taphonomy* 10(3–4):197–217
- Frank RD, Yakel E, Faniel IM (2015) Destruction/reconstruction: preservation of archaeological and zoological research data. *Arch Sci* 15(2):141–167. <https://doi.org/10.1007/s10502-014-9238-9>
- Gilbert MTP, Jenkins DL, Götherstrom A, Naveran N, Sanchez JJ, Hofreiter M, Thomsen PF, Binladen J, Higham TFG, Yohe RMII, Parr R, Cummings LS, Willerslev E (2008) DNA from pre-Clovis human coprolites in Oregon, North America. *Science* 320(5877):786–789. <https://doi.org/10.1126/science.1154116>
- Gill F, Crump M, Schouten R, Bull I (2009) Lipid biomarker analysis of *Nothotherium shastaensis* coprolite. *J Vertebr Paleontol* 29:105A
- Harrault L, Milek K, Jardé E, Jeanneau L, Derrien M, Anderson DG (2019) Faecal biomarkers can distinguish specific mammalian species in modern and past environments. *PLoS One* 14(2):e0211119. <https://doi.org/10.1371/journal.pone.0211119>
- Heizer RF (1963) The anthropology of prehistoric great basin human coprolites. In: Brothwell D, Higgs E (eds) *Science in Archaeology: a survey of progress and research*. Thames & Hudson, London, pp 244–250
- Hillson S (2005) *Teeth*, Second edn. Cambridge University Press, Cambridge
- Hollocher KT, Hollocher TC, Rigby JK Jr (2010) A phosphatic coprolite lacking diagenetic permineralization from the upper Cretaceous Hell Creek formation, northeastern Montana: importance of dietary calcium phosphate in preservation. *PALAIOS* 25(2):132–140. <https://doi.org/10.2110/palo.2008.p08-132r>
- Hunt AP, Chin K, Lockley MG (1994) The palaeobiology of vertebrate coprolites. In: Donovan SK (ed) *The Palaeobiology of Trace Fossils*. John Wiley & Sons, Chichester, pp 221–240
- Jenkins DL, Davis LG, Stafford TW Jr, Campos PF, Hockett B, Jones GT, Cummings LS, Yost C, Connolly TJ, Yohe RMII, Gibbons SC, Raghavan M, Rasmussen M, Paijmans JLA, Hofreiter M, Kemp BM, Barta JL, Monroe C, Gilbert MTP, Willerslev E (2012) Clovis age Western Stemmed projectile points and human coprolites at the Paisley Caves. *Science* 337(6091):223–228. <https://doi.org/10.1126/science.1218443>
- Lawrence MJ, Brown RW (1973) *Mammals of Britain: their tracks trails and signs*, revised edn. Blandford Press, London
- Maschner H, Chippindale C (2005) *Handbook of archaeological methods*. AltaMira Press, Oxford
- Milà J, Rasmussen BW, Lynnerup N (2012a) A coprolite in the MDCT-Scanner-internal architecture and bone contents revealed. In Hunt et al. (ed) *Vertebrate Coprolites*. New Mexico Museum of Natural History and Science Bulletin 57, Albuquerque NM, pp. 99–104
- Milà J, Rasmussen BW, Bonde N (2012b) Coprolites with prey remains and traces from coprophagous organisms from the lower cretaceous (late Berriasian) Jydegaard formation of Bornholm, Denmark. In Hunt et al. (ed) *Vertebrate Coprolites*. New Mexico Museum of Natural History and Science Bulletin 57, Albuquerque NM, pp. 235–240
- Payne S, Munson PJ (1985) Ruby and how many squirrels? The destruction of bones by dogs. In: Fieller NJR, Gilbertson DD, Ralph NGA (eds) *Palaeobiological investigations: research design, methods and data analysis*. British Archaeological Reports, Oxford, pp 31–40
- Perkins DN, Pappin DJC, Creasy DM, Cottrell JS (1999) Probability-based protein identification by searching sequence databases using mass spectrometry data. *Electrophoresis* 20:3551–3567. [https://doi.org/10.1002/\(SICI\)1522-2683\(19991201\)20:18<3551::AID-ELPS3551>3.0.CO;2-2](https://doi.org/10.1002/(SICI)1522-2683(19991201)20:18<3551::AID-ELPS3551>3.0.CO;2-2)
- Pesquero MD, Souza-Egipsy V, Alcalá L, Ascaso C, Fernández-Jalvo Y (2014) Calcium phosphate preservation of faecal bacterial negative moulds in hyaena coprolites. *Acta Palaeontol Pol* 59(4):997–1005. <https://doi.org/10.4202/app.2012.0067>
- Pettrigh RS, Fugassa MH (2017) Improved coprolite identification in Patagonian archaeological Contexts. *Quat Int* 438:90–93. <https://doi.org/10.1016/j.quaint.2017.03.006>
- Reinhard KJ, Bryant VM (1992) Coprolite analysis: a biological perspective on archaeology. *Archaeol Method Theory* 4:245–288. <https://digitalcommons.unl.edu/natresreinhard/35>
- Reinhard KJ (2000) Coprolite analysis: the analysis of ancient human feces for dietary data. In: Ellis L (ed) *Archaeological Method and Theory: An Encyclopedia*. University of Nebraska, Lincoln, pp 124–132
- Reinhard KJ, Ambler JR, Szuter CR (2007) Hunter-gatherer use of small animal food resources: coprolite evidence. *Papers Nat Resour* 73:416–428. <https://doi.org/10.1002/oa.883>
- Renfrew C, Bahn P (2012) *Archaeology: theories, methods and practice*, sixth edn. Thames & Hudson, London
- Romaniuk AA, Shepherd AN, Clarke DV, Sheridan AJ, Fraser S, Bartosiewicz L, Herman JS (2016) Rodents: food or pests in Neolithic Orkney. *Royal Society Open Sci* 3(10):160514. <https://doi.org/10.1098/rsos.160514>
- Rose FEN (1975) A note on the Orkney Vole. In: Goodier R (ed) *The natural environment of Orkney: proceedings of the Nature Conservancy Council Symposium Held in Edinburgh 26–27 November 1974*. Nature Conservancy Council, Edinburgh, pp 29–30
- Schmid E (1972) *Atlas of Animal Bones*. Elsevier Publishing Company, Amsterdam, London, New York
- Sharples NM (1984) Excavations at Pierowall Westray, Orkney. *Proc Soc Antiqu Scotl* 114:75–125
- Shepherd A (2016) Skara Brae life studies: overlaying the embedded images. In Hunter F, Sheridan A (ed) *Ancient lives: object, people and place in early Scotland*. Essays for David V Clarke on his 70th birthday. Sidestone Press, Leiden, pp. 213–232. <https://www.sidestone.com/books/ancient-lives>
- Sheridan A, Clarke D, Shepherd A (2013) Radiocarbon dates for Skara Brae, Orkney. *Discovery and excavation: Scotland* 13:204–205
- van der Sluis L, Hollund HI, Buckley M, De Louw PGB, Rijdsdijk KF, Kars H (2014) Combining histology, stable isotope analysis and ZooMS collagen fingerprinting to investigate the taphonomic history and dietary behaviour of extinct giant tortoises from the Mare aux Songes deposit on Mauritius. *Palaeogeography, Palaeoclimatology, Palaeoecology* 416: 80–91. <https://doi.org/10.1016/j.palaeo.2014.06.003>
- Wadsworth C, Procopio N, Anderung C, Carretero JM, Iriarte E, Valdiosera C, Elburg R, Penkman K, Buckley M (2017) Comparing ancient DNA survival and proteome content in 69 archaeological cattle tooth and bone samples from multiple European sites. *J Proteome* 158:1–8. <https://doi.org/10.1016/j.jprot.2017.01.004>
- Wang X, White SC, Balisi M, Biewer J, Sankey J, Garber D (2018) Tseng ZJ (2018) First bone-cracking dog coprolites provide new insight into bone consumption in Borophagus and their unique ecological niche. *eLife* 7:e34773. <https://doi.org/10.7554/eLife.34773>
- Wood JR, Wilmshurst JM (2016) A protocol for subsampling Late Quaternary coprolites for multi-proxy analysis. *Quat Sci Rev* 138: 1–5. <https://doi.org/10.1016/j.quascirev.2016.02.018>